

# Radio detections of the neutron star X-ray binaries 4U 1820-30 and Ser X-1 in soft X-ray states

S. Migliari<sup>1\*</sup>, R. P. Fender<sup>1†</sup>, M. Rupen<sup>2</sup>, S. Wachter<sup>3</sup>, P. G. Jonker<sup>4</sup>,  
J. Homan<sup>5</sup>, M. van der Klis<sup>1</sup>

<sup>1</sup> *Astronomical Institute ‘Anton Pannekoek’, University of Amsterdam, and Center for High Energy Astrophysics, Kruislaan 403, 1098 SJ, Amsterdam, The Netherlands.*

<sup>2</sup> *National Radio Astronomy Observatory, Socorro, NM 87801, USA*

<sup>3</sup> *SIRTF Science Center, California Institute of Technology, MS 220-6, Pasadena, CA 91125*

<sup>4</sup> *Institute of Astronomy, Madingley Road, CB3 0HA, Cambridge, UK*

<sup>5</sup> *MIT Center for Space Research, 77 Massachusetts Avenue, Cambridge, MA 02139*

30 July 2021

## ABSTRACT

We present the analysis of simultaneous X-ray (RXTE) and radio (VLA) observations of two atoll-type neutron star X-ray binaries: 4U 1820–30 and Ser X-1. Both sources were steadily in the soft (banana) X-ray state during the observations. We have detected the radio counterpart of 4U 1820–30 at 4.86 GHz and 8.46 GHz at a flux density of  $\sim 0.1$  mJy. This radio source is positionally coincident with the radio pulsar PSR 1820–30A. However, the pulsar’s radio emission falls rapidly with frequency ( $\propto \nu^{-3}$ ) and we argue that the X-ray binary’s radio emission is dominant above  $\sim 2$  GHz. Supporting this interpretation, comparison with previous observations reveals variability at the higher radio frequencies that is likely to be due to the X-ray binary. We have detected for the first time the radio counterpart of Ser X-1 at 8.46 GHz, also at a flux density of  $\sim 0.1$  mJy. The position of the radio counterpart has allowed us to unambiguously identify its optical counterpart. We briefly discuss similarities and differences between the disc-jet coupling in neutron star and black hole X-ray binaries. In particular, we draw attention to the fact that, contrary to other states, neutron star X-ray binaries seem to be more radio loud than persistent black hole candidates when the emission is ‘quenched’ in the soft state.

## Key words:

binaries: close – stars: neutron stars: individual: – ISM: jets and outflows radio continuum: stars

## 1 INTRODUCTION

Many works suggest that the radio emission in X-ray binaries, even when no spatial structure is resolved, originates in jet-like outflows (Hjellming & Han 1995; Falcke & Biermann 1996; Dhawan, Mirabel & Rodríguez 2000; Fomalont, Geldzahler & Bradshaw 2001; Fender 2004). A X-ray/radio correlation is therefore usually interpreted as a disc/jet coupling in the systems. In black hole candidate (BHC) X-ray binaries a connection between radio emission and X-ray emission is already clear. Studies of BHCs in the low/hard state showed a strong correlation between X-ray and radio

fluxes over more than three orders of magnitude in accretion rate (Hannikainen et al. 1998; Corbel et al. 2000; Corbel et al. 2003; Gallo, Fender & Pooley 2003). For X-ray luminosities greater than a few per cent Eddington, where the X-ray spectra soften dramatically, the radio emission seems to be ‘quenched’ (Fender et al. 1999; Corbel et al. 2001; Gallo et al. 2003).

Low magnetic field neutron star (NS) X-ray binaries have been classified, based on X-ray spectral and timing properties, in two distinct classes whose names recall the shape they trace in the colour-colour diagram (CD): Z-type and atoll-type (Hasinger & van der Klis 1989). The position of the source in the CD defines its X-ray state. In atoll sources the hardest X-ray state is called ‘island’ state and the softest ‘banana’ state (see Hasinger & van der Klis 1989

\* [migliari@science.uva.nl](mailto:migliari@science.uva.nl)

† [rpf@science.uva.nl](mailto:rpf@science.uva.nl)

for details). Atoll-type X-ray binaries in the hard state share many X-ray timing and spectral properties with BHCs in the low/hard state (e.g. van der Klis 1994). However, our understanding of the relation between radio activity and X-ray state in these NS sources remains sketchy. This is mainly due to the fact that their radio luminosities are significantly less than in BHs (Fender & Hendry 2000), resulting in a rather small number of atoll sources with identified radio counterparts (Hjellming & Han 1995; Berendsen et al. 2000). Recently, Migliari et al. (2003) found the first evidence for a disc-jet coupling in an atoll source, analysing simultaneous X-ray and radio observations of the NS X-ray binary 4U 1728–34, when the source was in the hard (i.e. mainly island) state. We found positive ranking correlations between the radio flux density and X-ray flux and between the radio flux density and X-ray timing features. We also confirmed quantitatively that in the hard state black hole binaries are  $\sim 30$  times more 'radio loud' than atoll-type NSs at a similar Eddington fraction (see also Fender & Kuulkers 2001).

In this paper we analyse simultaneous X-ray and radio observations of two atoll-type NS sources in the X-ray soft (i.e. middle-upper banana) state: 4U 1820–30 and Ser X-1 (4U 1837+04).

### 1.1 4U 1820–30

4U 1820–30 is a low-mass X-ray binary located in the globular cluster NGC 6624 (Giacconi et al. 1974). A distance of  $7.6 \pm 0.4$  kpc (Heasley et al. 2000) has been derived from optical observations. Grindlay et al. (1976) discovered thermonuclear X-ray bursts in the source, indicating a neutron star as compact object. From X-ray burst properties a distance of  $\sim 6.6$  kpc can be derived (Vacca, Lewin & van Paradijs 1986; see Kuulkers et al. 2003). Smale, Zhang & White (1997) reported the discovery of kHz QPOs in 4U 1820–30. A correlation between the frequency of the kHz QPOs and the position in the CD was found by Bloser et al. (2000). In particular, in 4U 1820–30 the kHz QPOs seem to be present while the source is in the lower banana state and absent when in the upper banana. The broadband 2–50 keV spectrum of the source is well fit with a typical model for atoll source in the soft state: a blackbody (or a multitemperature disc blackbody) plus a cutoff power law or with a Comptonisation model (e.g. *CompTT*: Titarchuck 1994) plus a blackbody component (e.g. Bloser et al. 2000). The radio source at the position of 4U 1820–30 was detected from observations with the Very Large Array (VLA) at 1.4 GHz by Geldzahler (1983) with a flux density of  $2.44 \pm 0.37$  mJy and then by Grindlay & Seaquist (1986) at the same frequency with a flux density of  $0.49 \pm 0.12$  mJy. The identification of this radio source as the radio counterpart of the X-ray binary is controversial. Johnston & Kulkarni (1992) first identified the radio source they found at 1.4 GHz at the position of the X-ray binary as the radio counterpart of 4U 1820–30. Later, based on the steepness of the spectrum of the radio source (a non-detection at 8.5 GHz with  $\text{rms} \sim 20 \mu\text{Jy}$ ; see also Biggs et al. 1994), they (Johnston & Kulkarni 1993) identified the radio source as a pulsar. The radio position of this pulsar, PSR 1820–30A (Biggs et al. 1990; Biggs et al. 1994; Stappers 1997) is coincident with the optical counterpart of the X-ray binary (Sosin & King 1995), and with the most recent VLA detection at 1.5 GHz

and 5 GHz (Fruchter & Goss 2000). These two sources are spatially unresolved. This makes the identification of the real origin of the observed radio emission difficult.

### 1.2 Ser X-1

Ser X-1 was discovered in X-rays in 1965 (Friedmann, Byram & Chubb 1967). The source shows thermonuclear X-ray bursts, reported for the first time by Swank et al. (1976). Ser X-1 is one of the three NS binary systems in which simultaneous X-ray and optical bursts have been observed (Hackwell et al. 1979). Christian & Swank (1997) derived a distance of  $\sim 8.4$  kpc from burst properties. The X-ray energy spectrum of the source is reasonably well fit with the same model used for 4U 1820–30: a soft component, blackbody or multicolor disc blackbody, and a Comptonised component (e.g. Oosterbroek et al. 2001). The optical counterpart was first identified as a blue star by Davidsen (1975). Subsequently, it turned out that the optical counterpart was in fact two unresolved stars (Thorstensen, Charles & Bowyer 1980). The two Davidsen stars are called DN (north) and DS (south), and DS (now called MM Ser) is the proposed optical counterpart (Thorstensen et al. 1980). Wachter (1997) found that DS is itself the superposition of two previously unresolved stars, DSw (west) and DSe (east), separated by  $1''$ . The brightest of the two stars (DSe) was suggested to be the real counterpart of Ser X-1 by Wachter (1997). Hynes et al. (2003) deblended the spectra of the DSe and DSw and found further spectral confirmation of Wachter (1997) suggestion. At radio wavelengths Grindlay & Seaquist (1986) reported upper limits of  $< 0.4$  mJy at 5 GHz.

## 2 OBSERVATIONS AND DATA ANALYSIS

We have analysed simultaneous radio and X-ray observations of 4U 1820–30 and Ser X-1 performed with the VLA and with the Rossi X-ray Timing Explorer (RXTE). The dates of the observations are shown in Table 1.

### 2.1 VLA

We have analysed seven observations of 4U 1820–30 (whose durations range from about 40 min to two hours) and one observation (of about five hours) of Ser X-1 with the VLA at 4.86 and 8.46 GHz. During the 4U 1820–30 observations the VLA was in B configuration, and during the Ser X-1 observation in A configuration. For 4U 1820–30 we have used 1331+305 (3C286) as the flux calibrator and 1820–254 (J2000 RA  $18^{\text{h}}20^{\text{m}}57^{\text{s}}.8487$  Dec.  $-25^{\circ}28'12''.587$ ) as the phase calibrator. For Ser X-1 we have used both 0137+331 (3C48) and 1331+305 (3C286) as flux calibrators and 1824+107 (J2000 RA  $18^{\text{h}}24^{\text{m}}02^{\text{s}}.8554$  Dec.  $-10^{\circ}44'23''.772$ ) as the phase calibrator. Flux densities of the two sources measured at both frequencies are shown in Table 1. Much of the data of 4U 1820–30 on MJD 52492 had to be discarded due to bad weather, leading to the larger errors in Table 1. The best-fit coordinates, from fits in the image plane assuming a Gaussian model, for the radio counterpart of 4U 1820–30 are J2000 RA  $18^{\text{h}}23^{\text{m}}40^{\text{s}}.4820 \pm 0^{\text{s}}.0088$  Dec.  $-30^{\circ}21'40''.12 \pm 0''.16$ , and for the radio counterpart of Ser X-1 are J2000 RA  $18^{\text{h}}39^{\text{m}}57^{\text{s}}.557 \pm 0^{\text{s}}.010$  Dec.

**Table 1.** Modified Julian Day (MJD), 2–10 keV unabsorbed flux ( $F_{2-10\text{keV}}$ ) in  $\text{erg s}^{-1} \text{cm}^{-2}$ , radio flux density at 4.86 GHz ( $F_{4.86\text{GHz}}$ ) and at 8.46 GHz ( $F_{8.46\text{GHz}}$ ) in mJy for seven VLA observations of 4U 1820–30 (five of which simultaneous with RXTE) and for one VLA observation (simultaneous with RXTE) of Ser X-1. Error bars are  $1\sigma$  errors.

MJD	$F_{2-10\text{keV}}$ ( $\text{erg s}^{-1} \text{cm}^{-2}$ )	$F_{4.86\text{GHz}}$ (mJy)	$F_{8.46\text{GHz}}$ (mJy)
4U 1820-30			
52480 <sup>a</sup>	$7.9 \times 10^{-9}$	$0.16 \pm 0.10$	$0.14 \pm 0.04$
52482	$8.7 \times 10^{-9}$	$0.13 \pm 0.10$	$0.08 \pm 0.04$
52484	$8.7 \times 10^{-9}$	$0.15 \pm 0.09$	$0.10 \pm 0.04$
52487	$9.0 \times 10^{-9}$	$0.17 \pm 0.09$	$0.10 \pm 0.04$
52489	$9.2 \times 10^{-9}$	$0.08 \pm 0.09$	$0.06 \pm 0.05$
52492 <sup>b,c</sup>	...	$0.09 \pm 0.16$	$0.04 \pm 0.06$
52494 <sup>b</sup>	...	$-0.07 \pm 0.10$	$0.09 \pm 0.04$
Averaged	$8.7 \times 10^{-9}$	$0.13 \pm 0.04$	$0.10 \pm 0.02$
Ser X-1			
52421	$4.4 \times 10^{-9}$	$0.05 \pm 0.04$	$0.08 \pm 0.02$

**a:** the 2–10 keV unabsorbed flux is the averaged flux of the four RXTE observations performed on MJD 52480; **b:** not simultaneous with RXTE; **c:** bad weather

+05°02′09″.50 ± 0″.14. The naturally-weighted synthesized beam width for the combined data of 4U 1820–30 is of  $3.49 \times 1.46$  arcsec in position angle  $-1.2^\circ$  at 5 GHz and of  $1.96 \times 0.80$  arcsec in position angle  $-2.2^\circ$  at 8 GHz, and for Ser X-1 is of  $1.51 \times 0.79$  arcsec in position angle  $+66.2^\circ$  at 5 GHz and of  $0.77 \times 0.46$  arcsec in position angle  $+67.1^\circ$  at 8.3 GHz. There is no evidence for any spatial extension to the radio counterparts of either source. Neither 4U 1820–30 nor Ser X-1 shows significant radio variability over the time of monitoring.

## 2.2 RXTE

For the RXTE observations we have used data from the Proportional Counter Array (PCA; for spectral and timing analysis) and the High Energy X-ray Timing Experiment (HEXTE; only for spectral analysis). We have used the PCA `Standard2` data of the proportional counter unit 2 (PCU2; on in all the observations) to produce the CD of all the RXTE observations of 4U 1820–30 and Ser X-1 available in the public archive. A soft colour and a hard colour are defined as the count rate ratio (3.5–6) keV/(2–3.5) keV and (9.7–16) keV/(6–9.7) keV, respectively. We have normalised the colours of 4U 1820–30 and Ser X-1 to the colours of the Crab calculated with the closest observation available to each observation analysed. Assuming the steadiness of the Crab energy spectrum, this normalisation allows us to compare observations in different epochs minimising shifts in the CD of instrumental origin. In Fig. 1 we show the mean colours (black dots) of each of the public RXTE observations of 4U 1820–30 (top panel) and Ser X-1 (bottom panel). The observations marked with open circles are simultaneous with radio (VLA) observations. We have analysed in detail (X-ray spectral and timing analysis) only these simultaneous radio/X-ray observations. The open squares mark

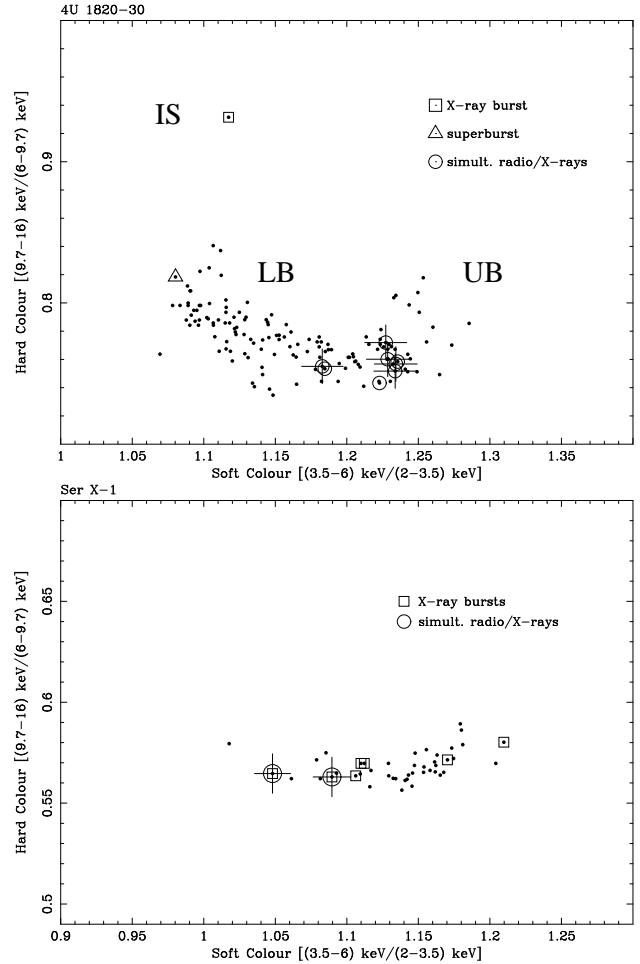


**Figure 1.** Mean colours (with PCU2 only) of each of all the observations of 4U 1820–30 (top panel) and Ser X-1 (bottom panel) in the RXTE public archive. The observations marked with open circles are simultaneous with radio (VLA) observations and those marked with open squares are the observations that show X-ray bursts. In 4U 1820–30 (top panel) the open triangle shows the observation in which the ‘superburst’ was discovered (Strohmayer & Brown 2000). Crosses indicate 90 per cent error bars.

the observations in which X-ray bursts are observed in the PCA light curve. In the CD of 4U 1820–30 (Fig. 1, top) the open triangle shows the observation in which the so-called ‘superburst’ was discovered (Strohmayer & Brown 2000).

### 2.2.1 Spectral analysis

For the spectral analysis we have used PCA `Standard2` and HEXTE `Standard Mode` data. For PCA data reduction we have subtracted the background estimated using `pcabckest` v3.0, produced the detector response matrix with `pcarsp` v8.0, and analysed the energy spectrum in the range 3–20 keV. For HEXTE data we extracted energy spectra (channels 15–61) from cluster A, subtracted the background, corrected for deadtime using the standard `FTOOLS` V5.2 procedures and analysed the spectra between 20 and 50 keV. A conservative systematic error of 0.75% was added to the PCA data to account for uncertainties in the calibration.

In the case of 4U 1820–30, all the 3–50 keV energy

spectra obtained simultaneously with radio observations are well fit with a CompTT model (Titarchuk 1994) corrected for photoelectric absorption (without any need for an extra blackbody components; see Blosler et al. 2000); in the worst case we obtain  $\chi_{re}^2 = 1.1$  with 49 *d.o.f.* ( $\chi_{re}^2 = \chi^2/d.o.f.$ ). The equivalent hydrogen column density  $N_H$  is fixed to  $3 \times 10^{21} \text{ cm}^{-2}$  (e.g. Blosler et al. 2000). Using this model we obtain (Wien) temperatures  $kT_0$  of the seed photons around 0.6 keV and temperatures of the plasma of about 2.5–3 keV, with a plasma optical depth  $\tau \sim 7$ .

For Ser X-1, using the same model that successfully fit the spectra of 4U 1820–30, i.e. CompTT corrected for photoelectric absorption ( $N_H$  was fixed to  $5 \times 10^{21} \text{ cm}^{-2}$ ; e.g. Oosterbroek et al. 2001), we cannot obtain a  $\chi_{re}^2$  less than 1.8 (50 *d.o.f.*). The energy spectrum shows an excess between 6–7 keV. Therefore we added a Gaussian emission line around 6.5 keV to the model obtaining a better fit with  $\chi_{re}^2 = 0.8$  (47 *d.o.f.*). The CompTT model fit gives parameters values similar to those found for 4U 1820–30 (i.e.  $kT_0 \sim 0.7$  keV, temperatures of the plasma of about 2.6 keV and  $\tau \sim 6$ ). In Table 1 we show the unabsorbed 2–10 keV fluxes of Ser X-1 and of 4U 1820–30 using the CompTT model (plus a Gaussian emission line in the case of Ser X-1).

### 2.2.2 Timing analysis

For the production of the power spectra we have used `event` data with a time resolution of 125  $\mu\text{s}$ . We rebinned the data in time to obtain a Nyquist frequency of 4096 Hz. For each observation we created power spectra from segments of 128s length, using Fast Fourier Transform techniques (van der Klis 1989 and references therein); we removed detector dropouts from the data, but no background subtraction was performed. No deadtime corrections were done before creating the power spectra. We averaged the power spectra and subtracted the Poisson noise spectrum applying the method of Zhang et al. (1995), shifted in power to match the spectrum between 3000 and 4000 Hz (see Klein-Wolt, Homan & van der Klis in prep.). The Leahy normalisation was applied (Leahy et al. 1983) and then we converted the power spectra to squared fractional rms. We have fitted the power spectra with a multi-Lorentzian model (e.g. Belloni, Psaltis & van der Klis 2002 and references therein), and plotted in the  $\nu P_\nu$  representation (with  $P_\nu$  the normalized power and  $\nu$  the frequency). We need two to four Lorentzians to fit the seven power spectra of 4U 1820–30: a broad Lorentzian to fit the very low frequency noise (VLFN), one or two Lorentzians around 10–20 Hz to fit the break of the peaked noise component ( $L_b$ ; see van Straaten, van der Klis & Méndez 2003 for details on terminology) and a higher frequency feature ( $L_h$ ). In one observation (MJD 52482, see Fig. 2) we also need one narrow Lorentzian to fit a QPO around 100 Hz ( $L_{hHz}$ ). We have fit the two power spectra of Ser X-1 with four Lorentzians: a broad Lorentzian for the VLFN, one at 15 Hz, one around 30 Hz and, only in one of the two observations (see Fig. 2) a narrow one at  $\sim 70$  Hz. The last three features are consistent with being identified either as  $L_b$ ,  $L_h$  and  $L_{hHz}$  (as in the 4U 1820–30 power spectrum), or  $L_{b2}$ ,  $L_b$  and  $L_h$ .

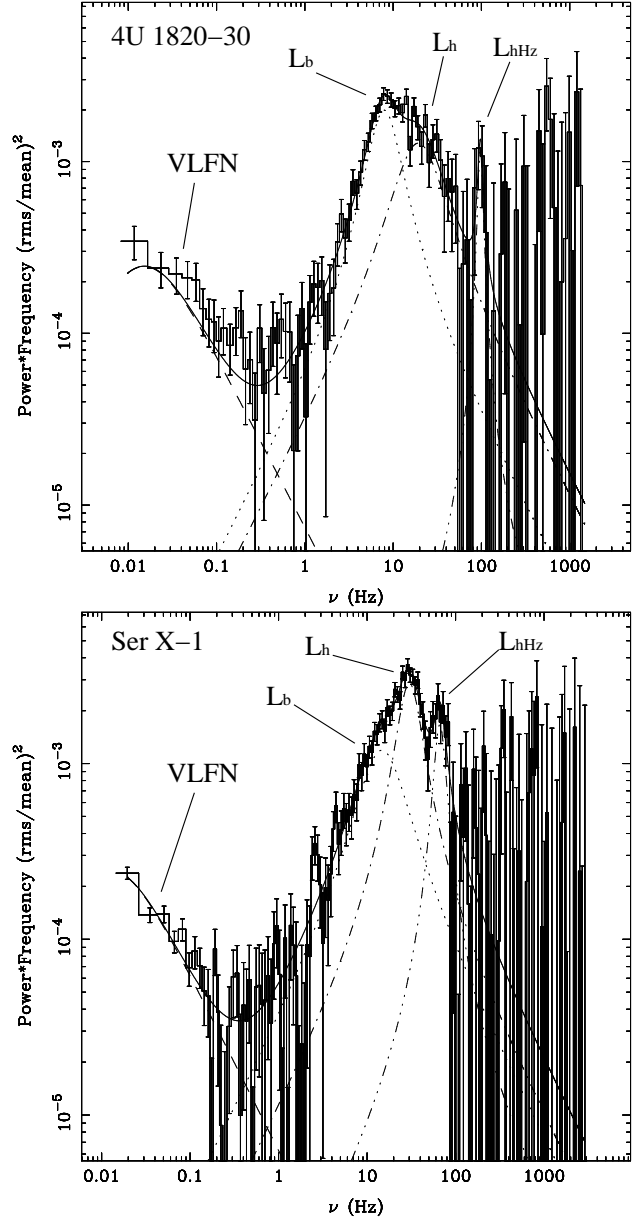


**Figure 2.** Power spectra of 4U 1820–30 on MJD 52482 (top panel) and of the second observation on MJD 52421 of Ser X-1 (bottom panel) with the best-fit model. Indicated are the four Lorentzian components fitting the very low frequency noise (VLFN), the break frequency ( $L_b$ ), the high frequency feature ( $L_h$ ) and the hecto Hz QPO ( $L_{hHz}$ ) (but see § 2.2.2).

## 3 RESULTS AND DISCUSSION

### 3.1 4U 1820–30

The CD of 4U 1820–30 (Fig. 1, top) shows that the simultaneous radio/X-ray observations are in the middle-upper banana. This is consistent with the power spectra characteristics: the presence of a VLFN (the integrated fractional rms of the fitting Lorentzian is  $\sim 3\%$ ) is typical of atoll sources in a soft X-ray state (i.e. middle-upper banana; see e.g. van Straaten et al. 2002); the absence of kHz QPOs characterises the power spectra of 4U 1820–30 in the middle-upper banana (Zhang et al. 1998; Blosler et al. 2000). The source is

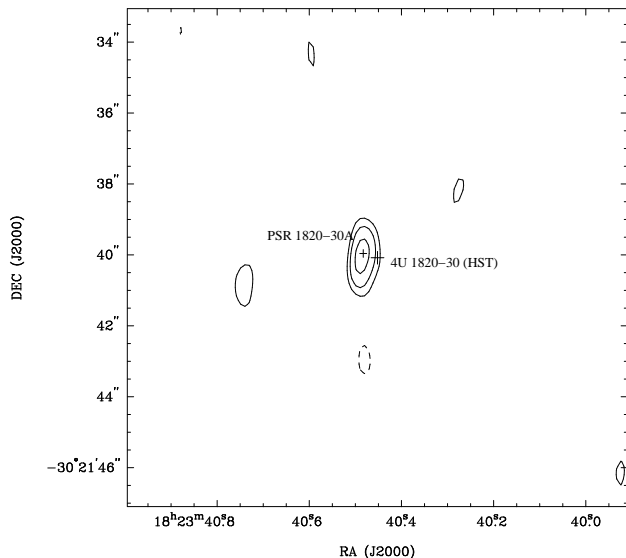


**Figure 3.** Naturally-weighted VLA radio contour plot of the averaged data of 4U 1820-30 at 8.46 GHz. We have chosen the contour interval as the rms of the image (0.015 mJy) and plot contours at  $-4$ ,  $-2.83$ ,  $2.828$ ,  $4$ ,  $5.657$  times the contour interval. The naturally-weighted synthesized beam width is of  $1.96 \times 0.80$  arcsec in position angle  $-2.2^\circ$ . The crosses indicate the Hubble Space Telescope (HST) position of the X-ray binary and the radio timing position of the pulsar PSR 1820-30A (see Table 2 and § 3.1). Sizes of crosses indicate  $1\sigma$  errors on the position.

detected at 8.46 GHz with a flux density of  $0.10 \pm 0.02$  mJy and marginally detected ( $\sim 3\sigma$ ) at 4.86 GHz with a flux density of  $0.13 \pm 0.04$  in the combined data (see Table 1). The mean (dual-frequency) radio spectrum has a spectral index  $\alpha = -0.48 \pm 0.62$  (where  $S_\nu \propto \nu^\alpha$  and  $S_\nu$  is the radio flux density at a frequency  $\nu$ ) consistent with either an optically thin or an optically thick spectrum. Biggs et al. (1994) reported radio detections (at 0.4 GHz, 0.6 GHz, 1.4 GHz and 1.7 GHz) of a pulsar, PSR 1820-30A. The position of this pulsar (see Stappers 1997 for a more accurate timing position) is coincident within  $2\sigma$  with the optical position of the X-ray binary 4U 1820-30 (Sosin & King 1995), and with the position of our radio detection (see Table 2 and Fig. 3). From the positions listed in Table 2 and using a distance to the sources of  $\sim 7$  kpc, we infer a lower limit on the physical separation between PSR 1820-30A and 4U 1820-30 of the order of few  $10^{16}$  cm.

In Fig. 3 we directly compare the positions of the sources plotting the positions listed in Table 2 on the VLA radio map. To do so, we have to take into account errors in the VLA coordinates due to the phase transfer. Therefore we have to increase the error bars when plotting other positions atop the VLA map: we added (in quadrature) to the non-VLA (i.e. the X-ray binary optical and the pulsar) positions an additional error of 0.098 arcsec. Moreover, in the case of the PSR 1820-30A (timing) position, there is a systematic offset due to the transfer from the timing frame to the VLA frame. Based on Fomalont et al. (1992), we add (in quadrature) an error of 0.005 arcsec in right ascension and 0.02 arcsec in declination to the pulsar position errors. Two other pulsars are identified in NGC 6624: PSR 1820-30B (Biggs et al. 1990; Biggs et al. 1994), which is too far

from the 4U 1820-30 optical position to contaminate our radio detection, and PSR 1820-30C (Chandler 2002), for which no coordinates are reported. In Fig. 3 we show the VLA radio contour map of 4U 1820-30 at 8.46 GHz. The crosses indicate the Hubble Space Telescope (HST) optical position of the X-ray binary (Sosin & King 1995) and the Parkes radio timing position of the pulsar PSR 1820-30A (Stappers 1997).

How do we know whether our radio detection comes from the X-ray binary or from the pulsar PSR 1820-30A, since they are positionally coincident? Fig. 4 shows the broadband (0.4 – 1.5 GHz) spectrum of the radio source. The dashed-dotted line is the best-fit power law of the data from Biggs et al. (1994) and the dashed line is the best-fit power law of the data from Toscano et al. (1998); both of these fits are for the low-frequency ( $< 2$  GHz) radio spectrum and are typical for radio pulsars. The radio spectrum of Toscano et al. (1998; the flatter of the two spectra in Fig. 4) is very steep, with  $\alpha \sim -2.9$ . The radio flux density at 1.4 GHz is  $\sim 0.7$  mJy. This spectrum would predict  $\sim 4 \mu\text{Jy}$  at 8.5 GHz, thirty times less than we detect (open diamonds in Fig. 4). The spectrum of the pulsar from Biggs et al. (1994), with  $\alpha \sim 3.7$ , is even more discrepant. The overall spectrum we observe in Fig. 4 seems to be the superposition of two main spectra, coming from two physically distinct but spatially unresolved sources. We suggest that below  $\sim 2$  GHz the pulsar dominates the radio emission with a steep spectrum, while the X-ray binary dominates the radio emission above  $\sim 2$  GHz with a flatter spectrum. Other radio detections above  $\sim 1.5$  GHz show large variability of the flux: at 4.8 GHz the flux density varies from a non-detection with an rms of 0.020 mJy (Johnston & Kulkarni 1993) to a detection of  $0.38 \pm 0.035$  mJy (Fruchter & Goss 1990). Previous dual-frequency radio detections at 1.5 GHz and 5 GHz (Fruchter & Goss 1990; Fruchter & Goss 2000; solid lines in Fig. 4) show flat spectra consistent with the spectrum we find with our detections at 5 GHz and 8.5 GHz. This further supports the idea that the X-ray binary dominates above  $\sim 1.5$  GHz and therefore suggests that flux variations in this frequency range are due to 4U 1820-30. The possibility that the flattening in the radio spectrum at high frequency is due to emission from a pulsar wind nebula (PWN) seems unlikely. First of all, the source shows a large radio flux variability (more than one order of magnitude at 1.4 GHz; see Fig. 4), unlike PWN. Moreover, either a relatively dense interstellar medium (ISM) and/or a high space velocity are required for the pulsar to power a wind nebula. The former condition makes globular clusters, lacking in dense ISM, an unlikely environment in which to find PWN (no PWN in globular clusters are, in fact, known). In the case of a high space velocity, the pulsar would have already escaped the central region of the cluster by now. The consistency with the Ser X-1 radio detection (e.g. similar radio luminosity at a similar X-ray luminosity and state) further supports our interpretation (see below).

### 3.2 Ser X-1

The CD of Ser X-1 (Fig. 1, bottom) indicates that the source is in the middle banana X-ray state during the radio observations. This is supported by the variability properties, e.g. the presence of a VLFN (rms  $\sim 3\%$ ), which are typi-

**Table 2.** Positions (with  $1\sigma$  errors) of the optical and radio counterparts of the X-ray binary 4U 1820–30 and the radio (timing) position of the pulsar PSR 1820–30A.

	Pos.	J2000	errors <sup>a</sup>
VLA source <sup>b</sup>	RA	18 <sup>h</sup> 23 <sup>m</sup> 40 <sup>s</sup> .4820	$\pm 0^s.0088$
	Dec	−30°21′40″.12	$\pm 0''.16$
4U 1820–30 (HST) <sup>c</sup>	RA	18 <sup>h</sup> 23 <sup>m</sup> 40 <sup>s</sup> .453	$\pm 0^s.012$
	Dec	−30°21′40″.08	$\pm 0''.15$
PSR 1820–30A <sup>d</sup>	RA	18 <sup>h</sup> 23 <sup>m</sup> 40 <sup>s</sup> .4840	$\pm 0^s.0006$
	Dec	−30°21′39″.96	$\pm 0''.05$

**a:** To directly compare the positions on the VLA map, as we do in Fig. 3, we have to add (in quadrature) an error of  $0''.098$  to the non-VLA positions, plus an additional error to the pulsar position due to a systematic offset between the timing and the VLA frame (see § 3.1). **b:** Our detection **c:** Sosin & King 1995 **d:** Stappers 1997

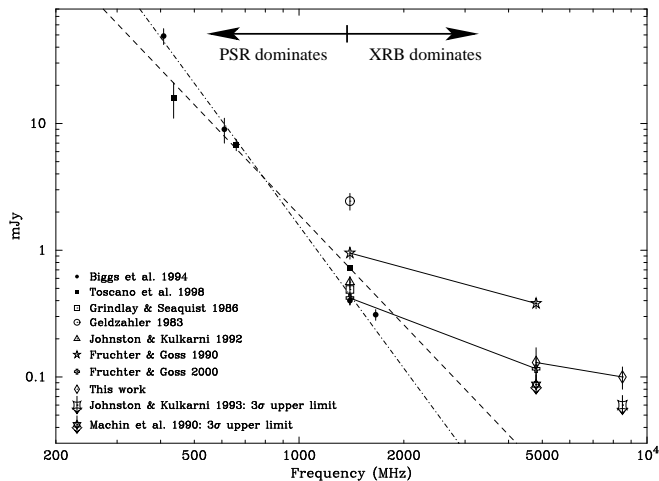


**Figure 4.** Radio flux density vs frequency of the published radio observations of the pulsar PSR 1820–30A and the X-ray binary 4U 1820–30. The dashed line is the best-fit power law of the pulsar observations from Toscano et al. (1998; black dots) and the dashed-dotted line is the best-fit power law of the pulsar observations from Biggs et al. (1994; black squares). The solid lines are the power law fits of the dual-frequency radio observations at 1.5 GHz and 5 GHz (open stars: Fruchter & Goss 1990; open crosses: Fruchter & Goss 2000) and at 5 GHz and 8.5 GHz (open diamonds: this work).

cal for an atoll source in its soft state (e.g. van Straaten et al. 2002). In both 4U 1820–30 and Ser X-1 we find similar spectral components in the energy spectra, which confirms that the sources are both in a similar (soft) state. We have detected for the first time the radio counterpart of Ser X-1, with a flux density at 8.46 GHz of  $0.08 \pm 0.02$  mJy (see Table 1). This detection is consistent with the previous upper limit of  $< 0.4$  mJy at 5 GHz of Grindlay & Seaquist (1986). Wachter (1997) showed that MM Ser, the optical counterpart of Ser X-1, is actually the superposition of two stars separated by  $1''$ . Therefore the position of the radio counterpart allows us to identify the correct optical counterpart. In Fig. 5 we show the optical image of the three stars (DN, DSe and DSw) with positions and errors marked with open circles. The optical image is a 400 sec R band

**Table 3.** Optical positions (with  $1\sigma$  errors) of the DN, DSe and DSw stars (open circles) and the position (with  $1\sigma$  errors) of the radio counterpart (cross) of the X-ray binary Ser X-1.

	Pos.	J2000	errors <sup>a</sup>
Ser X-1 (VLA)	RA	18 <sup>h</sup> 39 <sup>m</sup> 57 <sup>s</sup> .557	$\pm 0^s.010$
	Dec	+05°02′09″.50	$\pm 0''.14$
DN	RA	18 <sup>h</sup> 39 <sup>m</sup> 57 <sup>s</sup> .61	$\pm 0^s.02$
	Dec	+05°02′11″.67	$\pm 0''.36$
DSe	RA	18 <sup>h</sup> 39 <sup>m</sup> 57 <sup>s</sup> .56	$\pm 0^s.02$
	Dec	+05°02′09″.74	$\pm 0''.36$
DSw	RA	18 <sup>h</sup> 39 <sup>m</sup> 57 <sup>s</sup> .49	$\pm 0^s.02$
	Dec	+05°02′09″.51	$\pm 0''.36$

**a:** To directly compare the positions on the optical image, as we do in Fig. 5, we have to add (in quadrature) an error of  $0''.36$  to the VLA position of Ser X-1 (see § 3.2)

exposure obtained with the CTIO 0.9m telescope on 1996 July 11 (for details on the reduction and calibration of the image see Wachter 1997). An astrometric solution for the  $3' \times 3'$  frame was derived utilizing 40 stars from the USNO-A2.0 catalog and the IRAF task “cmap”. The errors on the optical positions are a combination of the uncertainties due to the USNO A-2.0 system ( $0''.3$ ) and to the transfer of that coordinate system onto the Ser X-1 frame ( $0''.2$ ). The cross indicates our VLA position (with  $1\sigma$  errors) of the radio counterpart. We clearly see that the radio position is coincident within uncertainties with DSe. From the spectral identification of Hynes et al. (2003) and our positional identification we can definitely confirm that DSe is MM Ser, the actual optical counterpart of Ser X-1.

### 3.3 Radio:X-ray correlation in X-ray binaries

The simultaneous radio and X-ray detections of 4U 1820–30 and Ser X-1 adds new information to the radio/X-ray relations in X-ray binaries. These two atoll sources are both steadily in the soft (banana) state. The radio emission of BHCs in the low/hard state increases as the X-ray flux increases and then decreases drastically (it is ‘quenched’) by a factor of  $> 50$ , when the source enters a softer (high/soft or intermediate) X-ray state. In 4U 1728–34 in the hard state (mostly island with two excursions to the lower banana) a similar correlation has been observed (Migliari et al. 2003). One data point (the one with the highest X-ray luminosity) lay off the correlation, possibly (even if, oddly, this observation is still in the island state) indicating a radio ‘quenching’. We have now detected the radio counterparts of two NS systems in the soft state (middle-upper banana, with X-ray luminosities higher than those of 4U 1728–34) at radio luminosities close to that found in 4U 1728–34 for its highest X-ray luminosity observation. However, in the case of these NS systems the reduction in radio luminosities between the brightest hard state and the soft state seems to be only of a factor of  $\sim 10$ . This indicates that *if* there is a radio ‘quenching’ also in atoll sources, this would be less extreme than in BHCs. Furthermore, if we compare the luminosities we have observed for these NS sources and the upper limits on the radio luminosities of the BHCs in the soft state (quenching), we note that in BHs the radio luminosity is lower than in

NSs. In fact, we have detected 4U 1820-30 and Ser X-1 at 8.5 GHz with a radio luminosity of  $\sim 5.0 \times 10^{28}$  erg s $^{-1}$  (using a distance of 7 kpc) and  $\sim 5.8 \times 10^{28}$  erg s $^{-1}$  (using a distance of 8.4 kpc), respectively. The BHC XTE 1550-564 when ‘quenched’ has a radio luminosity upper limit of  $< 1.8 \times 10^{28}$  erg s $^{-1}$  (measured at 8.5 GHz and using a distance to the source of 6 kpc; Corbel et al. 2002) and GX 339-4 of  $< 2.6 \times 10^{28}$  erg s $^{-1}$  (measured at 5 GHz and using a distance of 6 kpc; Fender et al. 1999). Therefore, NS X-ray binaries in the soft state (when the jet, at least for BHCs, seems to be suppressed) are more luminous in the radio band than BH X-ray binaries. This is contrary to other X-ray states, in which the BHCs are more radio loud, and seems to indicate that a ‘residual’ radio emission is present in the NS systems. This difference with BHCs might be related to the presence of a solid surface and/or to the NS magnetic field. Recent theoretical works (e.g. Meier 2001) seems to support the idea that an efficient jet-like outflow production is associated with a geometrically thick accretion disc (i.e. low/hard state in BHCs), while a suppression of the (observable) jet should happen when the disc become geometrically thin (i.e. high/soft state in BHCs). Speculating within this picture, assuming the same jet production processes in NS and BH X-ray binaries (see Fender et al., 2004) a possible explanation might be that the magnetic field of the NS could interact with the accretion disc, which in the softer states should be closer to the compact object, keeping the disc thick enough not to suppress completely the jet production mechanisms.

#### 4 CONCLUSIONS

We have detected two atoll-type neutron star X-ray binaries, 4U 1820-30 and Ser X-1, at radio wavelengths. In particular:

- We argue that we have detected the radio counterpart of 4U 1820-30, which can be spectrally distinguished from the positionally coincident radio pulsar PSR 1820-30A. The radio emission of the X-ray binary is dominant at higher frequencies, above  $\sim 2$  GHz and shows a flatter spectrum.
- We have detected for the first time the radio counterpart of Ser X-1; this radio detection allows us to identify star DSe as the optical counterpart of Ser X-1.
- Both 4U 1820-30 and Ser X-1 are detected at radio wavelengths while steadily in the banana (soft) state. This is different from 4U 1728-34 which has been detected at radio wavelengths in the banana state during transient excursions from the island.
- The radio luminosities in the soft state of 4U 1820-30 and Ser X-1 are higher than the radio luminosities in the soft state of BHCs (for which the jet is drastically suppressed). If the pattern of the radio flux vs. X-ray flux of atoll sources is analogous to BHCs, then radio ‘quenching’ in soft state of atoll sources does not seem to be as extreme as in BHCs.

#### ACKNOWLEDGEMENTS

SM and RPF would like to thank Ben Stappers for very useful discussions. The National Radio Astronomy Observatory is a facility of the National Science Foundation operated under cooperative agreement by Associated Universities, Inc.

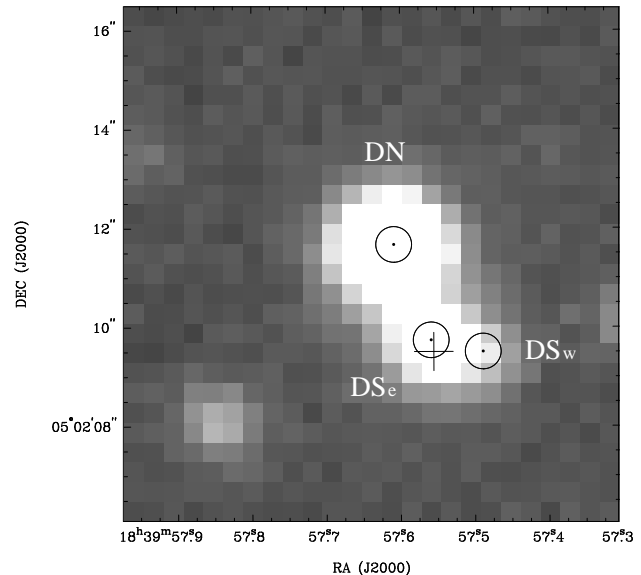


**Figure 5.** Portion of the optical ( $R$ -band) image of the field of MM Ser, with the three stars: DN, DSe and DSw (see Wachter 1997). The position (with  $1\sigma$  errors) of the three stars are marked with open circles; the position (with  $1\sigma$  errors) of the radio counterpart is indicated with a cross (see Table 3 and § 3.2).

#### REFERENCES

- Belloni T., Psaltis D., van der Klis M., 2002, ApJ, 572, 392  
 Berendsen S.G.H., Fender R.P., Kuulkers E., Heise J., van der Klis M., 2000, MNRAS, 318, 599  
 Biggs J.D., Lyne A.G., Manchester R.N., Ashworth M., 1990, IAU Circ. No. 4988  
 Biggs J.D., Bailes M., Lyne A.G., Goss W.M., Fruchter A.S., 1994, MNRAS, 267, 125  
 Bloser P.F., Grindlay J.E., Kaaret P., Zhang W., Smale A.P., Barret D., 2000, ApJ, 542, 1000  
 Chandler A.M., 2002, PhD thesis, <http://resolver.caltech.edu/CaltechETD:etd-01232003-213508>  
 Christian D.J., Swank J.H., 1997, ApJS, 109, 177  
 Corbel S., Fender R.P., Tzioumis A.K., Nowak M.A., McIntyre V., Durouchoux P., Sood R., 2000, A&A, 359, 251  
 Corbel S. et al., 2001, ApJ, 554, 43  
 Corbel S., Nowak M.A., Fender R.P., Tzioumis A.K., Markoff S., 2002, A&A, 400, 1007  
 Davidsen A.F. 1975, IAU Circ., 2824  
 Dhawan V., Mirabel I.F., Rodriguez L.F., 2000, ApJ, 543, 373  
 Falcke H., Biermann P.L., 1996, A&A, 308, 321  
 Fender R.P., Wu K., Johnston H., Tzioumis A., Jonker P.G., Spencer R., van der Klis M., 2004, Nature, 427, 222  
 Fender R.P., 2004, in ‘Compact Stellar X-ray Sources’, eds. W.H.G. Lewin and M. van der Klis, in press, (astro-ph/0303339)  
 Fender R.P., 2001, MNRAS, 322, 31  
 Fender R.P., Hendry M.A., 2000, MNRAS, 317, 1  
 Fender R.P., et al., 1999, ApJ, 519, L165  
 Fomalont E.B., Geldzahler B.J., Bradshaw C.F., 2001, ApJ, 558, 283  
 Fomalont E.B., Goss W.M., Lyne A.G., Manchester R.N., Justtanont K., 1992, MNRAS, 258, 497  
 Friedmann H., Byram E., Chubb T., 1967, Science, 156, 374  
 Fruchter A.S., Goss W.M., 2000, ApJ, 536, 865  
 Fruchter A.S., Goss W.M., 1990, ApJ, 365, L63  
 Gallo E., Fender R.P., Pooley G.G., 2003, MNRAS, 344, 60

- Giacconi R., Murray S., Gursky H., Kellogg E., Schreier E., Matilsky T., Koch D., Tananbaum H., 1974, *ApJS*, 27, 37
- Geldzahler B.J., *ApJ*, 1983, 264, L49
- Grindlay J., Gursky H., Schnopper H., Parsignault D.R., Heise J., Brinkman A.C., Schrijver J., 1976, *ApJ*, 205, L127
- Grindlay J.E., Seaquist E.R., 1986, *ApJ*, 310, 172
- Hackwell J.A., Grasdalen G.L., Gehrz R.D., Cominsky L., Lewin W.H.G., van Paradijs J., 1979, *ApJ*, 233, L115
- Hannikainen D.C., Hunstead R.W., Campbell-Wilson D., Sood R.K., 1998, *A&A*, 337,460
- Hasinger G., van der Klis M., 1989, *A&A*, 225, 79
- Heasley J.N., Janes K.A., Zinn R., Demarque P., Da Costa G.S., Christian C. A., 2000, *AJ*, 120, 879
- Hjellming R.M., Han X.H., 1995, in Lewin W.H.G., van Paradijs J., van den Heuvel E.P.J., eds, *X-ray binaries*, CUP, p.308
- Hynes R.I., Charles P.A., van Zyl L., Barnes A., Steeghs D., O'Brien K., Casares J., 2003, *MNRAS*, in press; *astro-ph/0310796*
- Johnston H.M., Kulkarni S.R., 1992, *ApJ*, 393, L17
- Johnston H.M., Kulkarni S.R., 1993, *A&A*, 280, 523
- Kuulkers E., den Hartog P.R., in 't Zand J.J.M., Verbunt F.W.M., Harris W.E., Cocchi M., 2003, *A&A*, 399, 663
- Leahy, D.A., Darbro, W., Elsner, R.F., Weisskopf, M.C., Kahn, S., Sutherland, P.G., Grindlay, J.E., 1983, *ApJ*, 266, 160
- Lewin W.H.G., Clark G.W., Doty J., 1976, *IAU Circ.*, 2922
- Liu Q.Z., van Paradijs J., van den Heuvel E.P.J., 2000, *A&AS*, 147, 25
- Liu Q.Z., van Paradijs J., van den Heuvel E.P.J., 2001, *A&A*, 368, 1021
- Machin G., Lehto H.J., McHardy I.M., Callanan P.J., Charles P.A., 1990, *MNRAS*, 246, 237
- Meier D.L., 2001, *ApJ*, 548, L9
- Migliari S., Fender R.P., Rupen M., Jonker P.G., Klein-Wolt M., Hjellming R.M., van der Klis M., *MNRAS*, 342, L67
- Miller, M.C., Lamb, F.K., Psaltis, D., 1998, *ApJ*, 508, 791
- Monet D. et al., 1998, *USNO-A V2.0, A Catalog of Astrometric Standards*, U.S. Naval Observatory Flagstaff Station (USNOFS) and Universities Space Research Association (USRA) stationed at USNOFS
- Oosterbroek T., Barret D., Guainazzi M., Ford E.C., 2001, *A&A*, 366, 138
- Penninx et al., 1988, *Nature*, 336, 146
- Smale A.P., Zhang W., White N.E., 1997, *ApJ*, 483, L119
- Sosin C., King I.R., 1995, *AJ*, 109, 639
- Stappers B.W., 1997, PhD thesis
- Strohmayer T.E., Brown E.F., *ApJ*, 566, 1045
- Swank J.H., Becker R.H., Pravdo S.H., Saba J.R., Serlemitsos P.J., 1976, *IAU Circ.*, 2963
- Titarchuk L., 1994, *ApJ*, 276, L41
- Thorstensen J.R., Charles P.A., Bowyer S., 1980, *ApJ*, 238, 964
- Toscano M., Bailes M., Manchester R.N., Sandhu J.S., 1998, *ApJ*, 506, 863
- Vacca W.D., Lewin W.H.G., van Paradijs J., 1986, *MNRAS*, 220, 339
- van Straaten S., van der Klis M., Di Salvo T., Belloni T., 2002, *ApJ*, 568, 912
- van Straaten S., van der Klis M., Méndez M., 2003, *ApJ*, 596, 1155
- Wachter S., 1997, *ApJ*, 490, 401
- Zhang W., Jahoda K., Swank J.H., Morgan E.H., Giles A.B., 1995, *ApJ*, 449, 930
- Zhang W., Smale A.P., Strohmayer T.E., Swank J.H., 1998, *ApJ*, 500, L171